

## Determining the effects of Ephrin Type-B Receptor 6 and Type-A Receptor 3 on facilitating colorectal epithelial cell malignant transformation

Jiaming WANG<sup>1,\*</sup>, Yan ZHANG<sup>1,\*</sup>, Jiaao MA<sup>1,\*</sup>, Cheng YANG<sup>1</sup>, Muhong WANG<sup>1</sup>, Jiachen LV<sup>1</sup>, Yihui WANG<sup>1</sup>, Dazhuang MIAO<sup>1</sup>, Yan WANG<sup>1</sup>, Mingqi LI<sup>1</sup>, Cuicui CHAI<sup>2</sup>, Shixiong JIANG<sup>1</sup>, Jinxue TONG<sup>1</sup>, Mingzhe LI<sup>2,\*</sup>, Zhiwei YU<sup>1,2,\*</sup>

<sup>1</sup>Department of Colorectal Surgery, Harbin Medical University Cancer Hospital, Harbin, China; <sup>2</sup>Digestive Disease Center, The Seventh Affiliated Hospital of Sun Yat-sen University, Shenzhen, China

\*Correspondence: 0697@hrbmu.edu.cn; jackmarx@163.com

\*Contributed equally to this work.

Received March 9, 2021 / Accepted April 22, 2021

Ephrin Type-A Receptor 3 (EphA3) and Ephrin Type-B Receptor 6 (EphB6) belong to the ephrin receptor group consisting of the largest subset of receptor tyrosine kinases (RTKs) and are essential for neurogenesis and embryogenesis. The current study aimed to evaluate their functional roles in transforming colorectal epithelial cells and dissect the underlying molecular mechanisms. We observed altered EphA3 and EphB6 expression in tumor tissues as compared to normal tissues in a tissue microarray study. Enforced EphB6 expression promoted IMCE cell proliferation, migration, and invasion *in vitro* and tumor formation in nude mice, with a stronger oncogenic activity than EphA3. Pathway analysis of differentially expressed genes from a gene microarray study provided important insight into potential mechanisms through which EphB6 may regulate the malignant transformation of colorectal epithelial cells. This study represents the first demonstration of EphB6 in enhancing colorectal epithelial cell transformation, suggesting its stipulative role in the early stage of colorectal tumorigenesis. Our findings primarily uncover novel biomarkers and therapeutic targets of colorectal cancer.

*Key words:* EphB6, EphA3, colorectal cancer, malignant transformation

Among the various types of cancer, colorectal cancer (CRC) has the second and third highest incidence among females and males, respectively. Its incidence has continually increased in recent years, with more than 1.8 million new cases being estimated globally in 2018 [1, 2]. Patients with early- and late-stage CRC showed 5-year survival rates of 90.3% and 12.0%, respectively [3]. Therefore, in CRC, early diagnosis is critical for effective interventions. CRC transformation is known to be driven by complex interactions between genetic and environmental factors, however, the exact mechanisms involved in this process remain poorly understood [4, 5]. Hence, there is an urgent need to discover diagnostic biomarkers of an early-stage CRC, which would contribute to establishing effective therapies.

Among the receptor tyrosine kinases (RTKs), the largest subfamily is the erythropoietin-producing hepatocellular (Eph) receptor group, which is further divided into the EphA1-10 and EphB1-6 subgroups, involved in the invasiveness during cancer progression [6, 7]. EphA3 was demonstrated to be a tumor suppressor in various circumstances [8–10], it was also found to exert oncogenic effects in several

solid and hematopoietic cancers [11]. Our previous study revealed that EphA3 could maintain tumor-initiating cells in CRC [12], while others reported its high mutation rate in CRC [13].

As a special member of the Eph receptor group, EphB6 lacks catalytic activity and has been identified as a tumor suppressor in melanoma, neuroblastoma, and non-small cell lung cancer [14–16]. Consistent with this, its downregulation was found to be associated with the increased invasiveness and aggressiveness of these cancers [17]. However, EphB6 has been poorly investigated in CRC and its function therein is largely unknown.

This study was established to determine the transformative potential of EphA3 and EphB6 in the colonic adenoma cell line IMCE (Immortomouse-Min Colonic Epithelial Cells ApcMin/+). Our data demonstrated that increased EphB6 expression contributed to cell proliferation *in vitro* and CRC initiation *in vivo* to a much greater extent than ectopic EphA3 expression. To further investigate the mechanism through which EphB6 promotes CRC transformation, we carried out microarray, proteomic, and bioinformatic

matic analyses. We herein demonstrated that EphB6 plays a crucial role in the PI3K-AKT and MAPK signaling, thereby providing new insights into the mechanisms regulating the initiation of CRC.

## Materials and methods

**Immunohistochemistry.** EphA3 and EphB6 antibodies were used in the immunohistochemical (IHC) analysis of a human tissue microarray to investigate their protein levels. The tissue samples in the microarray included 40 normal controls, 40 adenomas, 60 adenocarcinomas, and 60 metastatic lymph nodes. Immunoreactivity was scored as follows: 0 (as negative), 0–4% positive cells; 1, 5–24% positive cells; 2, 25–49% positive cells; 3, 50–100% positive cells. Staining intensity was scored as follows: 0, negative; 1, mild; 2, intermediate; 3, intense. Immunoreactivity and intensity scores were added to determine EphA3 and EphB6 expression levels; expression levels were as follows: low, total score 0–2; high, total score  $\geq 3$ .

**Mice and cell culture.** Prior to the experiments, all animal protocols were approved by the Institutional Animal Care and Use Committee (IACUC) of the Third Affiliated Hospital of Harbin Medical University. Throughout the experiment, the 5–6-week-old BALB/c-nu male mice were maintained in the experimental animal center (a pathogen-free environment), the Third Affiliated Hospital of Harbin Medical University.

The rat colorectal YAMC, IMCE, YAMC-Ras, and IMCE-Ras cells originated from the colonic epithelium of F1 immorto-ApcMin/+ mouse hybrids. Upon being maintained in a humidified incubator with 5% CO<sub>2</sub> at 37°C, the cells were cultured in RPMI 1640 supplemented with heat-inactivated fetal bovine serum (5%), 5 ng/ml selenium acid, 5 µg/ml transferrin, 100 U/ml penicillin/streptomycin, 5 U/ml murine IFN-γ, and 5 µg/ml insulin.

**Gene expression analysis.** TRIzol reagent (Invitrogen, Carlsbad, CA, USA) was used to extract total RNA from IMCE cells, of which the mRNAs were reverse-transcribed into cDNAs using the Superscript First-Strand Synthesis System (Invitrogen), in accordance with the manufacturer's protocol, using poly(dT) primer. Primers used to amplify the coding regions of the EphA3 and EphB6 were as follows (from 5' to 3'): EphA3, ACT GGA TCC ATG GAT TGT CAG CTC TCC ATC CTC CTC CTT CTC and ACT CTC GAG TCA cag atc ctc ttc tga gat gag ttt ttg ttc GAA CAC GGG AAC TGG GCC ATT CTT TGA TTG CG (the lower-case part encodes a MYC tag); EphB6, ACT GGA TCC ATG GTG TGT AGC CTA TGG GTG CTG C; and ACT GAT ATC TTA ctt gtc gtc atc ctt gta gtc ATC GAC CTC CAC TGA GCC CTG CTG (the lower-case part encodes a Flag tag). The housekeeping gene GAPDH was used as a reference with the PCR primers GCC AAA AGG GTC ATC ATC TC and GTA GAG GCA GGG ATG ATG TTC. The PCR protocol was as follows: 95°C for 2 min; 30 cycles of 95°C for 30 s, 55°C for 45 s, and 72°C for 1 min; and then

final elongation at 72°C for 15 min. The amplified EphA3-Myc and EphB6-Flag were individually subcloned into the pcDNA3 vector.

**Protein expression analysis.** Upon the preparation of IMCE cell lysates, the Bradford protein assay was used to quantify the protein concentrations. Sodium dodecyl sulfate-polyacrylamide gel electrophoresis (SDS-PAGE) was then used to separate the whole-cell lysates with an equal amount of proteins, followed by a transfer onto a nitrocellulose membrane for western blot analysis. Antibodies directed against Flag (cat#14793), Myc tag (cat#2278), vimentin (cat#3932), phospho-Erk1/2 (cat#4370), phospho-JNK (cat#4668), phospho-Akt (cat#9271), and anti-GAPDH (cat#5174) were purchased from Cell Signaling, while the β-actin antibody (cat#A1978) was from Sigma-Aldrich. Following washing and incubation with the secondary antibodies, a chemiluminescence system (Perkin-Elmer) was used to develop the blots. Quantity One software was used in the densitometric quantification of the bands in western blot analyses.

**Stable cell line generation.** Lipofectamine 2000 (cat#11668019; Invitrogen, Carlsbad, CA, USA) was used to individually transfect the EphA3 and EphB6 vectors into IMCE cells, in accordance with the manufacturer's instructions. Twenty-four hours after transfection, cell culture was initiated in a medium containing G418 (Sigma, St. Louis, MO, USA) at concentrations increasing from 200 to 800 µg/ml over the course of 2 weeks. G418-resistant clones were identified to establish stable cell lines. The expression of EphA3 or EphB6 was determined by western blotting with Myc or Flag tag antibody to screen for stable cell lines individually expressing these two proteins. The generated cell lines are hereafter referred to as IMCE-EphA3 and IMCE-EphB6. The cell line generated using an empty vector is called IMCE-neo.

**Cell viability assay.** To assess cell viability, the CellTiter 96<sup>®</sup> AQueous One Solution Cell Proliferation Assay (cat# G3582, CellTiter96; Promega, Madison, WI, USA) was used, according to the manufacturer's instructions. A spectrophotometer (UV5100; Metash Instruments Co., Ltd, Shanghai, China) was subsequently used to measure the optical density. Data are presented as mean ± standard error (SE). Each experiment was triplicated.

**Clonogenicity assay.** Using a two-layer soft-agar system, seeding of IMCE cells was performed at a density of 1×10<sup>3</sup> cells/well into six-well plates, as previously described [12]. Incubation of the plates was then performed for 3 weeks in a 37°C cell culture incubator, followed by staining using 0.5% crystal violet and counting the colonies with at least 50 cells. Experiments were performed in triplicate and repeated at least three times.

**Wound-healing assay.** Seeding of IMCE cells was performed at a density of 2×10<sup>5</sup> cells/well into 12-well plates in 500 µl of DMEM with 10% FCS. When cell confluence reached 100%, a pipette tip was used to create a scratch wound

in each well, and the width of each wound was demarcated. Cells were immediately washed with PBS to remove loose cells and debris from the culture. Plates were then incubated at 37°C for 24 h to allow wound healing, which was then visualized using an inverted microscope. Each experiment was triplicated and repeated at least three times.

**In vitro migration assays.** Briefly, a total of  $5 \times 10^4$  cells were seeded into the upper chamber of a 24-well Transwell filter insert (pore size: 8  $\mu\text{m}$ ; Costar, Cambridge, MA, USA), which contained 500  $\mu\text{l}$  of DMEM with 1% FCS, while the lower chamber contained 500  $\mu\text{l}$  of DMEM with 10% FCS. The migration of cells was allowed to continue for 24–36 h, followed by the removal of nonmigrating cells on the upper surface with a cotton swab. Filters were then placed into 4% formaldehyde for fixation, after which the cells were stained with 0.5% crystal violet. Cells were then counted in five fields using a light microscope. Each experiment was triplicated and repeated at least three times.

**Scanning electron microscopy.** The morphology of stably transfected IMCE cells was analyzed using scanning electron microscopy. Incubation of cells in 2.5% glutaraldehyde was performed for 24 h, followed by dehydration using graded concentrations of ethanol and then  $\text{CO}_2$ . Mounting of samples was subsequently performed on aluminum, after which sputter-coating with gold was carried out, followed by analysis using a scanning electron microscope (JSM-7500F; JEOL, Tokyo, Japan) to visualize cell morphology.

**In vivo tumorigenesis assays.** To evaluate tumorigenesis *in vivo*, the flanks of nude mice were subcutaneously injected with  $8 \times 10^8$  IMCE cells as follows: Group A) IMCE-neo cells (negative control); Group B) IMCE-EphA3 cells; and Group C) IMCE-EphB6 cells. Each group consisted of 10 mice. Tumors were allowed to grow for 4 weeks, and then tumor volumes ( $V$ ,  $\text{cm}^3$ ) were calculated ( $V = 1 \times w \times h \times 0.5236$ ) using caliper-measured tumor length ( $l$ ), width ( $w$ ), and height ( $h$ ).

**Gene expression microarray analysis.** To establish profiles of the differentially expressed genes, IMCE-neo, IMCE-EphA3, and IMCE-EphB6 cells were analyzed using an  $8 \times 60\text{K}$  lncRNA Expression Array (Arraystar, Rockville, MD, USA). The mRNA microarray contained 23,420 probes for 17,298 genes. The lncRNA microarray included 34,735 probes. We defined a fold change of expression of  $\geq 1.5$  as indicative of a gene or lncRNA differentially expressed between IMCE-EphA3 and IMCE-EphB6 cells. We next used the human RefSeq reference genome (hg19) to determine potential target genes of the lncRNAs. Genes located within the region 500 kb upstream of the transcription start site of a given lncRNA were considered as its potential target.

**Bioinformatic analysis of differentially expressed genes and lncRNAs.** For Gene Ontology (GO) and Kyoto Encyclopedia of Genes and Genomes (KEGG) functional enrichment analysis, we used DAVID Functional Annotation Bioinformatics Microarray Analysis (<http://david.abcc.ncifcrf.gov/home.jsp>) on the differentially expressed genes and candi-

date target genes of the differentially expressed lncRNAs, respectively. Statistically significant differences in functional classes and pathways were determined using Fisher's exact test. We used the EnrichmentMap plug-in in Cytoscape to perform GO\_BP term enrichment analysis. To determine the relationship between significantly enriched functional classes and KEGG pathways, we used the EnrichmentMap plug-in in Cytoscape software to analyze enrichment results. Network nodes were differentially expressed mRNA-enriched GO terms and KEGG pathways, and node sizes were where the number of differentially expressed mRNAs was proportional. The edges of the network indicated that the nodes contained the same mRNA, the greater the number of shared mRNAs, the greater the width of the sides is.

**Protein-protein interaction subnetwork construction.** To create an integrated protein-protein interaction (PPI) network using Cytoscape (<http://www.cytoscape.org>), we used the following databases: the Biological General Repository for Interaction Datasets (BioGRID), the Biomolecular Interaction Network Database (BIND), the Human Protein Reference Database (HPRD), the Database of Interacting Proteins (DIP), the Molecular Interaction Database (MINT), PDZBase (a PPI database for PDZ domains), the Mammalian PPI Database of the Munich Information Center on Protein Sequences (MIPS), and Reactome. Seed genes were determined by common mRNAs and lncRNA candidate target genes. These seed genes as well as lncRNA candidate target genes and genes connected to the seed genes were then used to populate the sub-network.

**Statistical analysis.** In all of the statistical analyses, SAS software (version 9.2) was used. To determine the statistical significance of differences between groups, either paired Student's t-test or chi-squared ( $\chi^2$ ) test was used. One-way ANOVA was used for comparing multiple groups. A p-value  $< 0.05$  indicates a statistically significant difference.

## Results

**Expression of EphA3 and EphB6 in colorectal tissues and colorectal epithelial cell lines.** We first carried out immunohistochemical studies to evaluate EphA3 and EphB6 expression in colorectal tissues in a tissue microarray and observed their upregulation as CRC progressed toward an adenocarcinoma. Strong EphB6 staining was detected in most adenoma tissues, but only in some cancer tissues. In metastatic lymph nodes, EphB6 protein expression was found to be reduced compared with that in primary tumors. Weak EphB6 staining was also detected at crypt bases in normal tissues. Both EphA3 and EphB6 were highly expressed in adenomas (Figure 1A). High EphB6 protein expression was present in 26.7% (16/60) of tumor tissues, 82.5% (33/40) of adenoma tissues, and 12.5% (5/40) of normal tissues. The rate of high EphB6 expression in samples of metastatic lymph nodes (20.0%, 12/60) was lower than that in tumor tissues (26.7%, 16/60; Figure 1B).

**Stable expression of Eph in IMCE cells.** Using RT-PCR analysis, we discovered low endogenous EphA3 and EphB6 expression in IMCE cells; however, we found that they were expressed at relatively high levels in malignant YAMC-Ras and IMCE-Ras cell lines (Figure 1C). Given our observation of low endogenous EphA3 and EphB6 expression in IMCE cells, we next sought to determine whether enforced expression of these proteins could transform colorectal epithelial cells. For this purpose, we first constructed stable cell lines by individually transfecting pcDNA3-EphA3-Myc, pcDNA3-EphB6-Flag, and an empty vector into IMCE cells, followed by antibiotic selection for stable clones. The generated stable cell lines were named IMCE-EphA3, IMCE-EphB6, and IMCE-neo, respectively, and their expression of EphA3-Myc and EphB6-Flag was confirmed by western blot analysis (Figure 1D).

**EphA3 and EphB6 promoted colorectal epithelial cell transformation *in vitro*.** Upon using MTT assays to evaluate

cell proliferation, we are unable to find significant differences between IMCE-EphA3 and IMCE-neo cells, while ectopic IMCE-EphB6 cells showed substantially increased cell proliferation compared with IMCE-neo cells ( $p < 0.05$ , Figure 1E). In colony formation assays, IMCE-EphA3 and particularly IMCE-EphB6 cells formed more colonies than the control cells (Figure 1F), indicating that these two proteins could confer the transformative capacity to colorectal epithelial cells.

**EphA3 and EphB6 promoted colorectal epithelial cell motility.** Next, in wound-healing and Transwell assays, we discovered that both EphA3 and EphB6 could promote the migration of IMCE cells compared with the control cells. Notably, IMCE-EphB6 cells showed much more pronounced enhancement in the wound-healing and Transwell migration assays than IMCE-EphA3 cells ( $p < 0.05$ , Figures 2A, 2B). Furthermore, using scanning electron microscopy (SEM), we observed marked morphological alterations of IMCE-EphA3

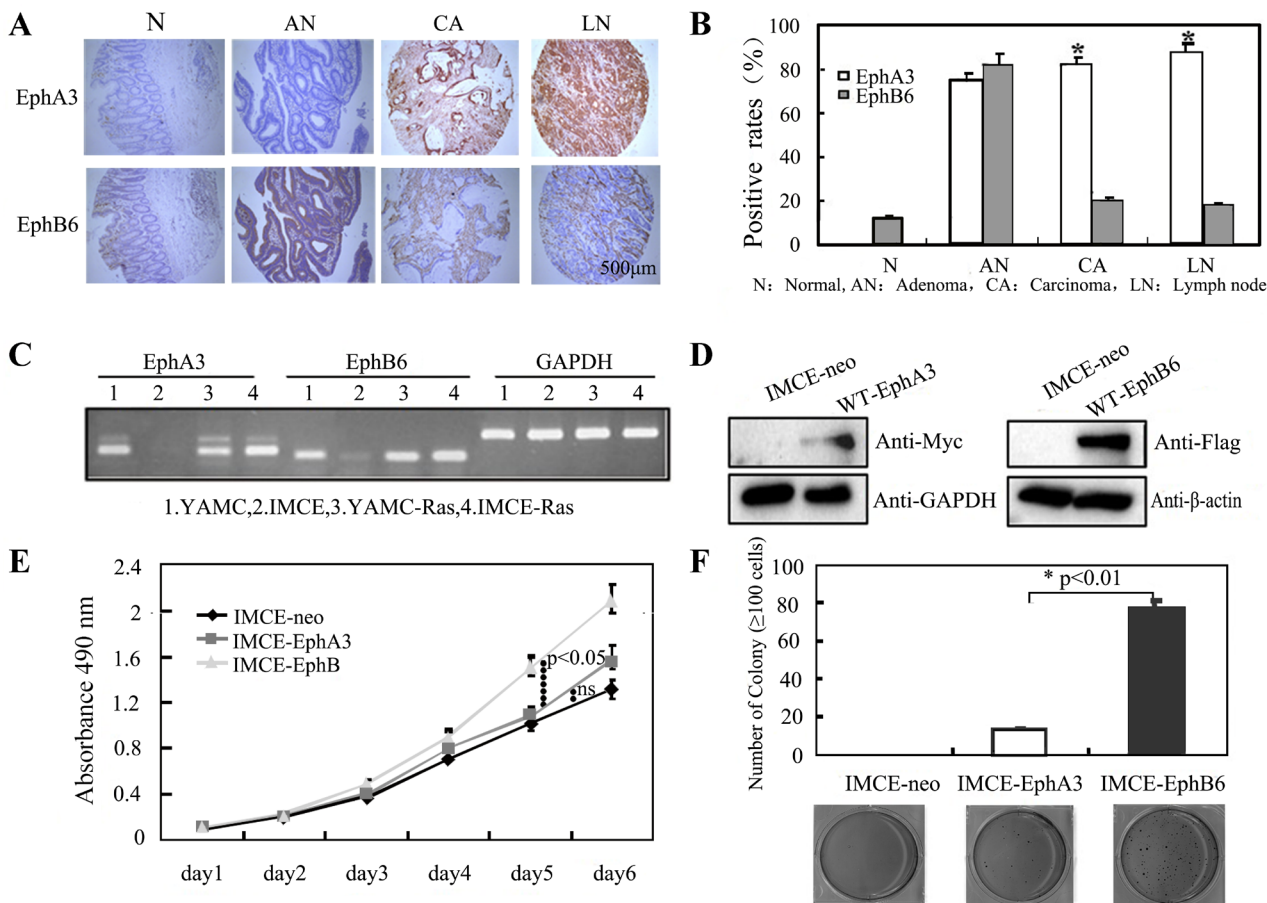


**Figure 1.** The expression of EphA3 and EphB6 in adenoma tissues and their roles in colony formation of colorectal epithelial cells. **A**) Immunohistochemical staining of EphA3 and EphB6 in normal mucosa (N), adenoma (AN), adenocarcinoma (CA), and metastatic lymph node (LN) obtained from patients with colorectal cancer. **B**) Quantification of EphA3 and EphB6 expression based on the analysis of **A**. Data of quantitative analyses are shown as mean  $\pm$  SD ( $n=3$ ). \*,  $p < 0.01$ . **C**) RT-PCR analysis of EphA3 and EphB6 mRNA levels in rat colorectal cells. YAMC: immorto-min F1, IMCE: immorto-min F1 with APC<sup>Min/+</sup>, YAMC-Ras: Ras-transgenic YAMC, IMCE-Ras: Ras-transgenic+APC<sup>Min/+</sup>. **D**) Western blot analysis of EphA3 and EphB6 proteins. **E**, **F**) MTT assays and colony formation assays of IMCE-EphA3 and IMCE-EphB6 cells. Data are shown as mean  $\pm$  SD ( $n=3$ ). ns: not significant.

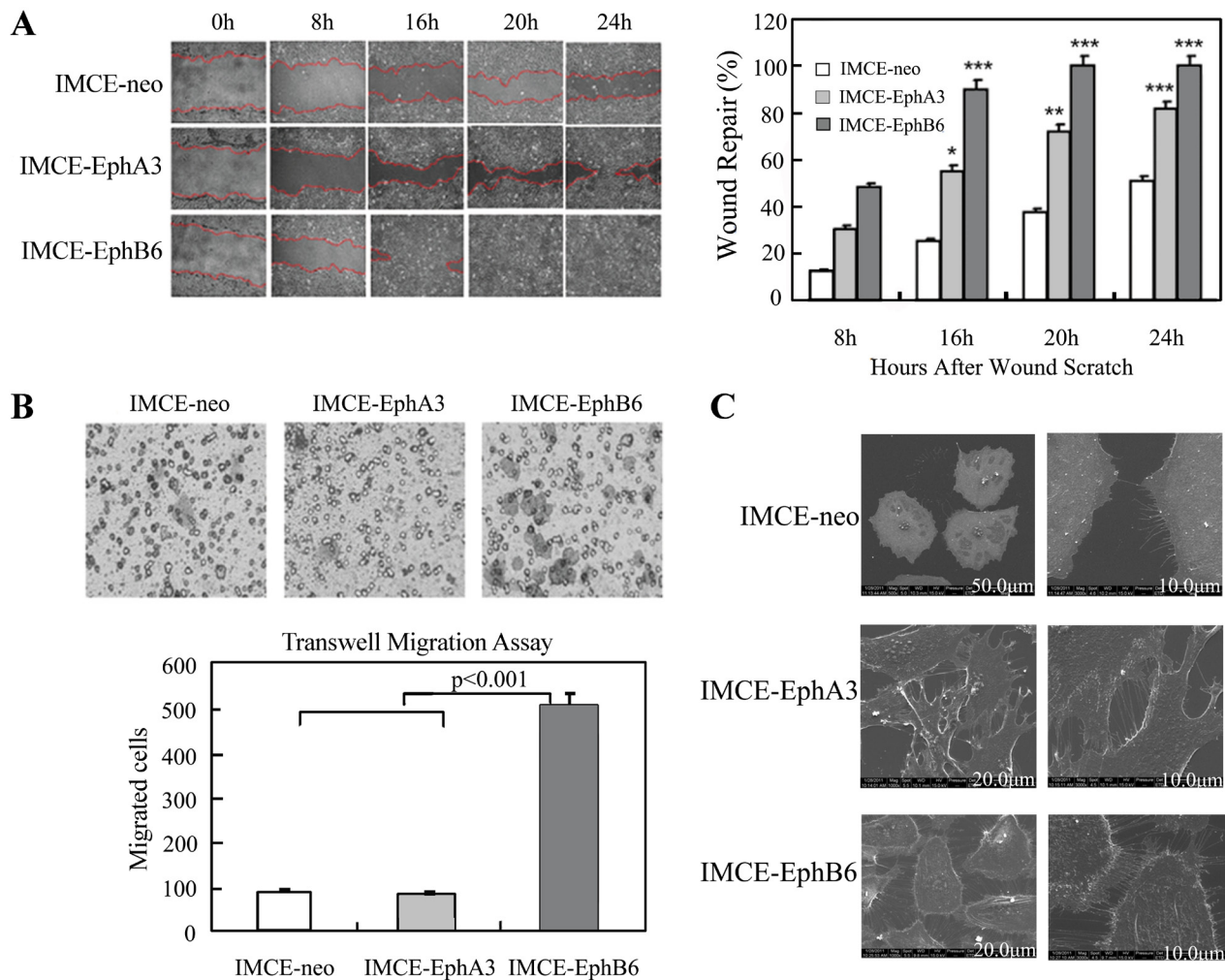


**Figure 2.** Effects of EphA3 and EphB6 on migration and invasion of colorectal epithelial cells. **A)** Wound-healing assays to evaluate migration rates. Data of quantitative analyses are shown as mean  $\pm$  SD (n=3). \* $p < 0.05$ , \*\* $p < 0.01$ , \*\*\* $p < 0.001$  **B)** Transwell assays to determine invasiveness of the IMCE-neo, IMCE-EphA3, and IMCE-EphB6 cells. Three representative images are shown. Data of quantitative analyses are shown as mean  $\pm$  SD (n=3). **C)** SEM analysis of the morphology of the IMCE-neo, IMCE-EphA3, and IMCE-EphB6 cells as described in the Materials and Methods section.

and IMCE-EphB6 cells in comparison to the IMCE-neo cells, including increased numbers of membrane ruffles and lamellipodia in IMCE-EphA3 cells and more filopodia in IMCE-EphB6 cells (Figure 2C). Taken together, these findings indicated that EphB6 and, to a lesser extent, EphA3 could promote colorectal cell motility, one of the characteristics of tumor cells.

**EphA3 and EphB6 promoted colorectal epithelial cell tumorigenesis *in vivo*.** Given that EphA3 and EphB6 conferred tumorigenic properties on IMCE cells *in vitro*, we investigated whether they could promote tumorigenesis *in vivo*. For this purpose, we employed a xenograft mouse model by individually inoculating IMCE-EphA3, IMCE-EphB6, and IMCE-neo cells into the flanks of athymic nude mice, with 10 mice in each group. Within 13 days post-inoculation, we observed tumors in 7 of the 10 mice injected with IMCE-

EphB6 cells. In contrast, mice injected with IMCE-EphA3 cells did not form any palpable tumors in this time period, but tumors started to be detectable after day 13, suggesting longer latency of tumor formation than for the IMCE-EphB6 cells. No tumor formation was observed in the mice inoculated with IMCE-neo cells (Figures 3A and B). Furthermore, the tumors in the EphB6 mice grew significantly larger than those in the EphA3 mice ( $p < 0.05$ , Figure 3C).

Tumorigenesis is particularly characterized by the dysregulation of cell proliferation. In view of this, we subsequently investigated the expression of proliferating cell nuclear antigen (PCNA), a marker of proliferating cells, in the xenograft tumors. In the immunohistochemical studies, we observed a PCNA signal in infiltrating lymphocytes in mice injected with IMCE-EphA3 and IMCE-EphB6 cells. Consistent with the difference in tumor size, the PCNA staining in

the EphB6 mice had a higher intensity than that in the EphA3 mice (Figures 3D, 3E).

**mRNAs and lncRNAs differentially expressed between IMCE-EphA3 and IMCE-EphB6 cells.** To provide mechanistic insight into how EphA3 and EphB6 could promote colorectal cell tumorigenicity, we compared mRNA and lncRNA expression profiles between the stable cell lines IMCE-EphA3 and IMCE-EphB6, using gene expression microarray analysis. While the mRNA expression patterns were generally highly similar between these two cell lines (Figure 4A), we observed 185 downregulated and 111 upregulated genes (fold change  $\geq 1.5$ ), and 250 downregulated and 231 upregulated lncRNAs (fold change  $\geq 1.5$ ) in the IMCE-EphB6 cells relative to the levels in the IMCE-EphA3 cells (Figures 4B, 4C).

To identify genes particularly associated with the obtained lncRNAs, we applied the GO and KEGG analyses. According to our results, cell morphogenetic formation in differentiation, regulation of cysteine-type endopeptidase activity

during apoptosis, and modulation of cellular metabolic processes are particularly associated with the candidate target genes. Eight pathways, such as the PI3K-AKT and MAPK signaling pathways, were particularly strongly linked to these genes (Figure 5A). To obtain an understanding of the cytoplasmic signaling used by Ephs to promote cell proliferation in tumorigenesis, we assessed their effects on essential signaling pathways. Although our findings revealed that the activating phosphorylation of Akt kinases was enhanced by EphA3 and EphB6, they did not appear to influence the phosphorylation of Erk1/2 and JNK. Given the association of EMT with the malignant transformation from normal epithelial cells to cancer cells, we next focused on whether Ephs affected the expression of the EMT marker vimentin, which is usually found in mesenchymal cells and promotes EMT. Our experiment indicated that EphB6 promoted vimentin expression (Figure 5D).

To determine the functional relationships between differentially expressed mRNA-enriched GO terms and

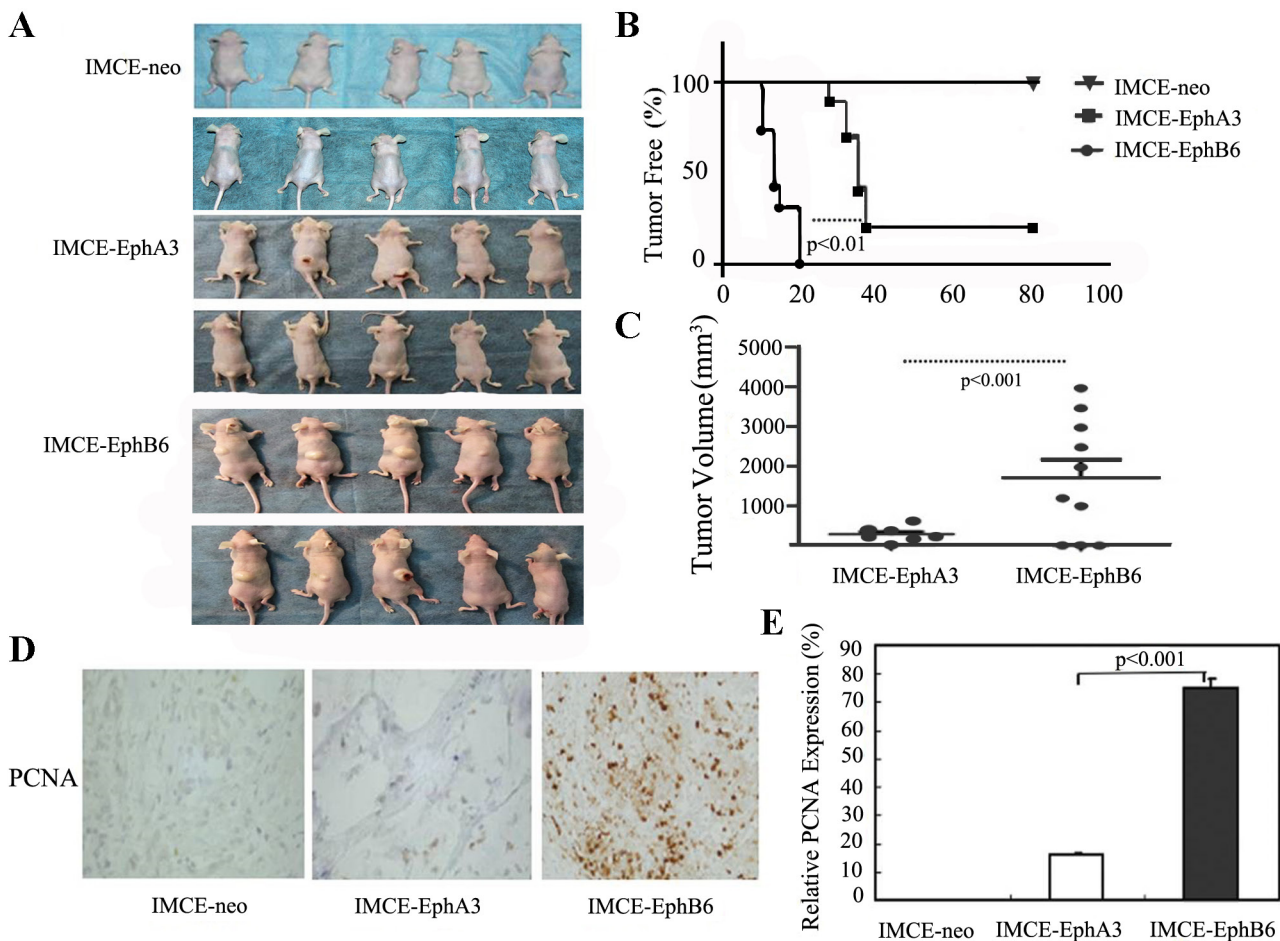


**Figure 3.** Xenograft mouse study to evaluate the effects of EphA3 and EphB6 on tumor formation. A) Nude mouse xenograft tumor formation study. The IMCE-neo, IMCE-EphA3, and IMCE-EphB6 cells were subcutaneously inoculated into the flanks of the athymic nude mice and the mice were sacrificed at 80 days after the inoculation. B) Tumor-free survival curves. C) Tumor volumes of the mice in the three groups. D) Representative images of PCNA staining of xenografts. E) The quantitation in the three groups. Data are shown as mean  $\pm$  SD (n=3). Scale bar = 20  $\mu$ m.

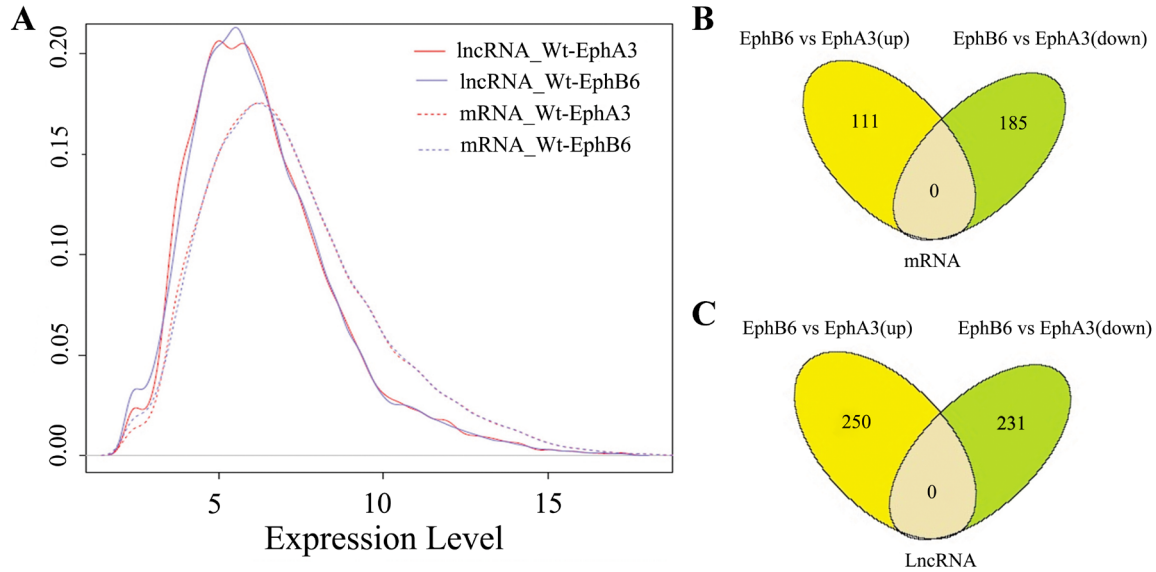


**Figure 4.** Global mRNA and lncRNA expression were subjected to microarray profiling. A) The global expression levels of mRNA and lncRNA in the cells were quantified. Circos v0.62 was used to profile the changes of global mRNA and lncRNA expression in the vector control, IMCE-EphA3, and IMCE-EphB6 cells. B, C) DAVID Functional Annotation Bioinformatics Microarray Analysis was used to identify 111 upregulated and 185 downregulated genes associated with tumorigenicity (B), and 250 upregulated and 231 downregulated lncRNAs associated with tumorigenicity (C).

KEGG pathways, we constructed an enrichment-responsive network with 113 nodes ( $p < 0.05$ ) and 1,392 edges, of which the red nodes were much more significant ( $p < 0.005$ ), including the HSA04151:PI3K-AKT signaling pathway (Figure 5B). The largest network was randomly walked and identified based on the relevance scores. Seven potential mRNA-lncRNA interaction pairs were identified, namely, RELA-ENST00000531155, IL6-ENST00000422542, IKBKB-ENST00000520890, TNF-NR\_002812, IFNAR1-NR\_038974, IFNAR2-NR\_038974, and JAK1-ENST00000447748 (Figure 5C).

## Discussion

Numerous studies have indicated the oncogenic activities of Ephs and ephrins in human cancers [7, 18]. Unfortunately, few studies have been performed on the roles of most Eph RTK group members, particularly EphA3 and EphB6, in CRC [19]. The current study represents a step toward filling this information gap. In this study, we demonstrated the overexpression of EphA3 protein in human tissue specimens from colorectal cancer and showed that its ectopic expression in IMCE cells prompted colorectal epithelial cells to undergo malignant transformation, albeit to a modest extent, *in vitro* and *in vivo*, as we previously reported [9]. Our EphB6 immunohistochemistry data showed that its staining intensity was first greatly increased in the progression from normal status to adenoma. Although this has not been reported previously, it is consistent with previous findings on other Eph subgroup members including EphA1, EphA2,

EphB1, EphB2, and EphB4 [6, 7, 18–20]. Moreover, in the progression of carcinoma to lymph node metastasis, EphB6 was found to show a stepwise decrease, while EphA3 exhibited a gradually increasing trend, suggesting that EphB6, but not EphA3, plays an oncogenic role at the early stage of colorectal cancer.

Our data demonstrated that enforced EphB6 expression promoted the proliferation, migration, and invasion of IMCE cells *in vitro*, along with tumor formation in nude mice. This suggested the potential oncogenic role played by EphB6 at the early stage of colorectal cancer. However, to date, no reports have been published about EphB6's role during tumor initiation. Nonetheless, studies focusing on other solid tumors, including non-small cell lung cancer, melanoma, and prostate cancer, reported that EphB6 acted as a tumor suppressor [14, 17, 21]. In clinical studies, it was also shown that EphB6 expression was decreased in CRC compared with the levels in adenoma and normal tissues, indicating that the loss of EphB6 contributed to the metastasis of colorectal cancer [22, 23]. Clinical evidence suggested that EphB6 shifted its function to a tumor suppressor in later stages of colorectal cancer. Our tissue microarray data revealed a significant reduction of EphB6 expression in the process of carcinoma progression to lymph node metastasis, confirming the phenomenon in later-stage colorectal cancer. The findings suggested that EphB6 acted as an oncogenic promoter in the early stage of colorectal cancer but then changed to a tumor-suppressive regulator. Thus, the loss of EphB6 expression in the late stage of tumor development,

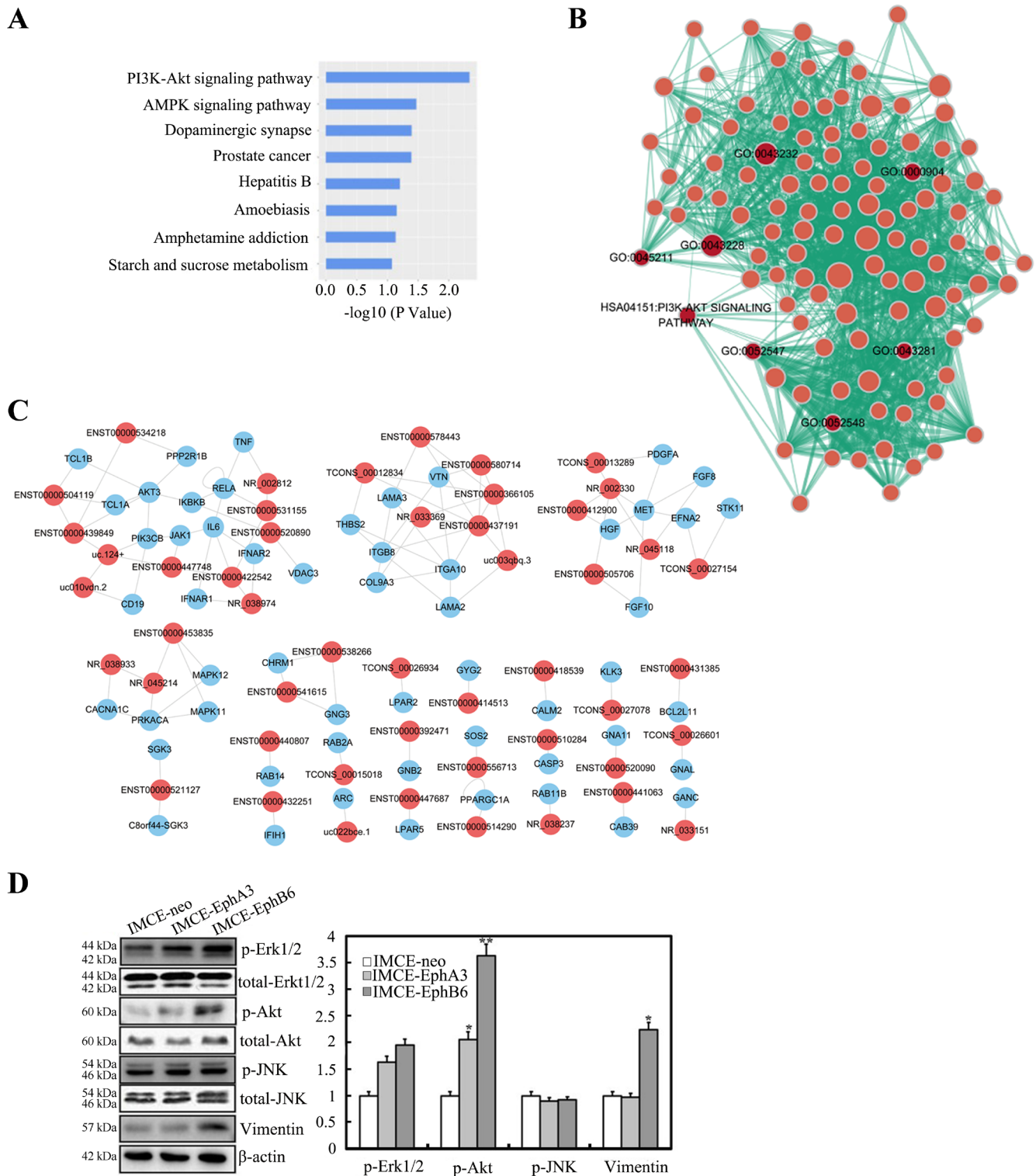


**Figure 5.** The functions particularly associated with the mRNAs differentially expressed between IMCE-EphA3 and IMCE-EphB6 cells. GO and KEGG enrichment analyses were applied to the host genes or the genes adjacent to the lncRNAs. A) The genes adjacent to the upregulated lncRNAs were enriched in eight gene pathways. B) An enrichment-responsive network of 113 nodes and 1,392 edges. C) The mRNA-lncRNA interaction network in EphA3 versus EphB6. The blue nodes denote mRNAs and the red nodes denote lncRNAs. D) An EMT marker, vimentin, and phosphorylation of Erk, Akt, and JNK kinases were assessed by western blot. Quantification for bands in the western blot was carried out by the Quantity One software. Data of quantitative analyses are shown as mean  $\pm$  SD (n=3). \*p<0.01, \*\*p<0.001.

possibly through epigenetic silencing, may facilitate tumor cell migration and metastasis [14, 19, 21].

EphB6 expression has been shown to be associated with poor overall survival in those with tongue squamous cell carcinoma and malignant thyroid lesions [24, 25]. A recent report also described a complex effect of EphB6 in regulating the initiation of triple-negative breast cancer [26], indicating that EphB6 plays various roles in different human malignancies. Intriguingly, Matsuoka *et al.* demonstrated that cell adhesion and migration were positively and negatively regulated by EphB6, respectively, showing that EphB6 exerts biphasic functions in the transition from oncogenic promotion to tumor suppression [27]. Thus, EphB6 may play different roles in a context-dependent manner and produce opposite responses in cell migration/invasion against different molecular backgrounds, or at different levels of its expression or signaling at different stages of malignancy. Our study represents the first demonstration that ectopic EphB6 expression can promote the malignant transformation of colonic adenoma cells.

In the current study, we explored downstream signaling events affected by ectopically expressed EphA3 and EphB6 in colorectal epithelial cells. The mRNAs and lncRNAs differentially expressed between EphA3- and EphB6-expressing IMCE cells were particularly associated with the PI3K-AKT and MAPK pathways, both of which regulate cell proliferation and differentiation. By western blot analysis, we also demonstrated that EphB6 increased the activation of phosphorylation of Erk1/2 and Akt kinases, as reported in a study on triple-negative breast cancer [27]. As these pathways and processes are known to affect oncogenic potential, these findings provide insight into the molecular mechanisms through which EphB6 promotes oncogenesis in colorectal cells. However, additional investigations are needed to delineate the molecular mechanisms responsible for EphB6-mediated oncogenic activity in CRC.

In our interaction network, seven potential mRNA-lncRNA interaction pairs were identified, six of which (RELA, IL6, IKBKB, TNF, IFNAR1, and IFNAR2) are important factors in immunological processes. Investigations have also shown that EphB6 could play a key role in immunological processes and particularly T-cell functions. EphB6 actually exerts adverse effects on the immune system and suppresses T-cell activity; the lack of EphB6 in these cells leads to inappropriately large numbers of T cells in the germinal centers resulting from relaxed repulsion of T follicular helper cells [28]. Loss of T-cell activity resulting from the presence of EphB6 in patients with tongue squamous cell carcinoma and malignant thyroid lesions resulted in a decreased ability to eliminate malignant cells [24, 25]. However, the current study has the potential limitation that only cases at the early stages of colorectal cancer were included. There is a need for further studies of the expression of EphB6 protein and mRNA in the late stages of colorectal cancer and in metastatic colorectal cancer tissues,

to provide further insight into the oncogenic mechanisms of EphB6 in CRC, and also its function in immunological processes. There is a need for careful evaluation to recognize the patterns and roles of EphB6 expression during CRC progression, which is essential for rationally targeting CRC with Eph-specific therapies.

Both EphA3 and EphB6 could promote the proliferation and migration of colorectal tumor cells. EphB6 enhanced the early-stage colorectal epithelial cell transformation and exhibited stronger oncogenic activity than EphA3. Thus, EphB6 expression may serve as a new marker and a potential therapeutic target of CRC at an early stage. Our data provide insights into the clinical diagnosis of CRC and early interventions to treat CRC patients.

**Acknowledgments:** This study was funded by the National Natural Science Foundation of China (No. 81272703); the Natural Science Foundation of Heilongjiang Province (No. QC08C56); the Free Exploration Foundation of Science, Technology and Innovation Commission of Shenzhen Municipality (No. JCYJ2018307151238174); and the Science and Technology Planning Project of Guangdong Province (No. 2017A020215014). The authors are grateful to Zhenfeng Zhang (Ireland Cancer Center, Case Western Reserve University, Cleveland, USA) who kindly donated to them the EphA3 and EphB6 expression vectors.

## References

- [1] BRAY F, FERLAY J, SOERJOMATARAM I, SIEGEL RL, TORRE LA *et al.* Global cancer statistics 2018: GLOBOCAN estimates of incidence and mortality worldwide for 36 cancers in 185 countries. *CA Cancer J Clin* 2018; 68: 394–424. <https://doi.org/10.3322/caac.21492>
- [2] DEKKER E, TANIS PJ, VLEUGELS JLA, KASI PM, WALLACE MB. Colorectal cancer. *Lancet* 2019; 394: 1467–1480. [https://doi.org/10.1016/S0140-6736\(19\)32319-0](https://doi.org/10.1016/S0140-6736(19)32319-0)
- [3] SIEGEL R, DESANTIS C, JEMAL A. Colorectal cancer statistics, 2014. *CA Cancer J Clin* 2014; 64: 104–17. <https://doi.org/10.3322/caac.21220>
- [4] STOFFEL EM, MURPHY CC. Epidemiology and Mechanisms of the Increasing Incidence of Colon and Rectal Cancers in Young Adults. *Gastroenterology* 2020; 158: 341–353. <https://doi.org/10.1053/j.gastro.2019.07.055>
- [5] MARKOWITZ SD, BERTAGNOLLI MM. Molecular origins of cancer: Molecular basis of colorectal cancer. *N Engl J Med* 2009; 361: 2449–2460. <https://doi.org/10.1056/NEJMr0804588>
- [6] TAYLOR H, CAMPBELL J, NOBES CD. Ephs and ephrins. *Curr Biol* 2017; 27: R90–R95. <https://doi.org/10.1016/j.cub.2017.01.003>
- [7] KOU CJ, KANDPAL RP. Differential Expression Patterns of Eph Receptors and Ephrin Ligands in Human Cancers. *Biomed Res Int* 2018; 2018: 7390104. <https://doi.org/10.1155/2018/7390104>

- [8] CHEN X, LU B, MA Q, JI CD, LI JZ. EphA3 inhibits migration and invasion of esophageal cancer cells by activating the mesenchymalepithelial transition process. *Int J Oncol* 2019; 54: 722–732. <https://doi.org/10.3892/ijo.2018.4639>
- [9] ZHUANG G, SONG W, AMATO K, HWANG Y, LEE K et al. Effects of cancer-associated EPHA3 mutations on lung cancer. *J Natl Cancer Inst* 2012; 104: 1182–1197. <https://doi.org/10.1093/jnci/djs297>
- [10] LISABETH EM, FERNANDEZ C, PASQUALE EB. Cancer somatic mutations disrupt functions of the EphA3 receptor tyrosine kinase through multiple mechanisms. *Biochemistry* 2012; 51: 1464–1475. <https://doi.org/10.1021/bi2014079>
- [11] JANES PW, SLAPE CI, FARNSWORTH RH, ATAPATTU L, SCOTT AM et al. EphA3 biology and cancer. *Growth Factors* 2014; 32: 176–189. <https://doi.org/10.3109/08977194.2014.982276>
- [12] LI M, YANG C, LIU X, YUAN L, ZHANG F et al. EphA3 promotes malignant transformation of colorectal epithelial cells by upregulating oncogenic pathways. *Cancer Lett* 2016; 383: 195–203. <https://doi.org/10.1016/j.canlet.2016.10.004>
- [13] SJOBLOM T, JONES S, WOOD LD, PARSONS DW, LIN J et al. The consensus coding sequences of human breast and colorectal cancers. *Science* 2006; 314: 268–274. <https://doi.org/10.1126/science.1133427>
- [14] YU J, BULK E, JI P, HASCHER A, TANG M et al. The EPHB6 receptor tyrosine kinase is a metastasis suppressor that is frequently silenced by promoter DNA hypermethylation in non-small cell lung cancer. *Clin Cancer Res* 2010; 16: 2275–2283. <https://doi.org/10.1158/1078-0432.CCR-09-2000>
- [15] HAFNER C, BATAILLE F, MEYER S, BECKER B, ROESCH A et al. Loss of EphB6 expression in metastatic melanoma. *Int J Oncol* 2003; 23: 1553–1559. <https://doi.org/10.3892/ijo.23.6.1553>
- [16] TANG XX, ZHAO H, ROBINSON ME, COHEN B, CNAAN A et al. Implications of EPHB6, EFNB2, and EFNB3 expressions in human neuroblastoma. *Proc Natl Acad Sci U S A* 2000; 97: 10936–10941. <https://doi.org/10.1073/pnas.190123297>
- [17] BAILEY CM, KULESA PM. Dynamic interactions between cancer cells and the embryonic microenvironment regulate cell invasion and reveal EphB6 as a metastasis suppressor. *Mol Cancer Res* 2014; 12: 1303–1313. <https://doi.org/10.1158/1541-7786.MCR-13-0673>
- [18] CASTANO J, DAVALOS V, SCHWARTZ S JR., ARANGO D. EPH receptors in cancer. *Histol Histopathol* 2008; 23: 1011–1023. <https://doi.org/10.14670/HH-23.1011>
- [19] HERATH NI, BOYD AW. The role of Eph receptors and ephrin ligands in colorectal cancer. *Int J Cancer* 2010; 126: 2003–2011. <https://doi.org/10.1002/ijc.25147>
- [20] XU D, YUAN L, LIU X, LI M, ZHANG F et al. EphB6 overexpression and Apc mutation together promote colorectal cancer. *Oncotarget* 2016; 7: 31111–31121. <https://doi.org/10.18632/oncotarget.9080>
- [21] MOHAMED ER, NOGUCHI M, HAMED AR, ELDAH-SHOURY MZ, HAMMADY AR et al. Reduced expression of erythropoietin-producing hepatocyte B6 receptor tyrosine kinase in prostate cancer. *Oncol Lett* 2015; 9: 1672–1676. <https://doi.org/10.3892/ol.2015.2925>
- [22] PENG L, TU P, WANG X, SHI S, ZHOU X et al. Loss of EphB6 protein expression in human colorectal cancer correlates with poor prognosis. *J Mol Histol* 2014; 45: 555–563. <https://doi.org/10.1007/s10735-014-9577-0>
- [23] MATEO-LOZANO S, BAZZOCCO S, RODRIGUES P, MAZZOLINI R, ANDRETTA E et al. Loss of the EPH receptor B6 contributes to colorectal cancer metastasis. *Sci Rep* 2017; 7: 43702. <https://doi.org/10.1038/srep43702>
- [24] DONG Y, PAN J, NI Y, HUANG X, CHEN X et al. High expression of EphB6 protein in tongue squamous cell carcinoma is associated with a poor outcome. *Int J Clin Exp Pathol* 2015; 8: 11428–11433. <https://www.ncbi.nlm.nih.gov/pmc/articles/PMC4637686/>
- [25] GIAGINIS C, ALEXANDROU P, POULAKI E, DELLADETSIMA I, TROUNGOS C et al. Clinical Significance of EphB4 and EphB6 Expression in Human Malignant and Benign Thyroid Lesions. *Pathol Oncol Res* 2016; 22: 269–275. <https://doi.org/10.1007/s12253-014-9879-2>
- [26] TOOSI BM, EL ZAWILY A, TRUITT L, SHANNON M, ALLONBY O et al. EPHB6 augments both development and drug sensitivity of triple-negative breast cancer tumours. *Oncogene* 2018; 37: 4073–4093. <https://doi.org/10.1038/s41388-018-0228-x>
- [27] MATSUOKA H, OBAMA H, KELLY ML, MATSUI T, NAKAMOTO M. Biphasic functions of the kinase-defective Ephb6 receptor in cell adhesion and migration. *J Biol Chem* 2005; 280: 29355–29363. <https://doi.org/10.1074/jbc.M500010200>
- [28] LU P, SHIH C, QI H. Ephrin B1-mediated repulsion and signaling control germinal center T cell territoriality and function. *Science* 2017; 356: eaai9264. <https://doi.org/10.1126/science.aai9264>